Preliminary Results of Satellite Radar Differential Interferometry for the Co-seismic Deformation of the 12 May 2008 Ms8.0 Wenchuan Earthquake

Linlin Ge, Kui Zhang, Alex Ng, Yusen Dong, Hsing-chung Chang, Chris Rizos

Cooperative Research Centre for Spatial Information School of Surveying & Spatial Information Systems
The University of New South Wales Sydney, NSW 2052 AUSTRALIA
E-mail: l.ge@unsw.edu.au

Abstract
Satellite differential SAR interferometry has been widely accepted as a powerful tool to map co-, post- and inter-seismic deformation since its successful application to the 1992 Landers Earthquake. As soon as the Ms8.0 Wenchuan Earthquake occurred on 12 May 2008 in the Sichuan Province of southwestern China, the Japan Aerospace Exploration Agency tasked its Advanced Land Observing Satellite (ALOS) to respond to the disaster by collecting images. This paper presents the preliminary DInSAR results of co-seismic deformation of the quake observed from two satellite paths of the onboard ALOS/PALSAR sensor with post-seismic images acquired on 19 and 24 May. Results from pixel offset analysis and difference of coherence will also be discussed. The radar mapping is still on-going because the ruptured seismic fault is more than 300km in length. Each swath of the PALSAR fine beam covers only about a 75km segment of the fault, and it takes 46 days for ALOS to revisit the same site.
Keywords
Sichuan Earthquake, SAR, ALOS/PALSAR, co-seismic deformation

I. INTRODUCTION

The devastating Ms8.0 Wenchuan Earthquake that struck China's southwestern Sichuan province occurred at 14:28:01. 42 UTC on 12 May 2008 in an area that is deforming as a result of the collision between two tectonic plates, the Indo-Australian plate and the Eurasian plate. As of 7 June 2008, it is estimated that 69,134 people were killed as a direct result of the quake(CEA, 2008). Since records were kept, there have been eight major earthquakes with magnitude larger than 7.0 within 200km of the current epicentre, with the Ms 7.5 in 1933 being the largest (CSIN, 2008).

ALOS, the Advanced Land Observing Satellite, is a follow-on Japanese satellite mission to the JERS-1 and the Advanced Earth Observing Satellite (ADEOS) missions. ALOS was launched on 24 January 2006 from the Tanegashima Space Centre by the Japan Aerospace Exploration Agency. The satellite is designed to provide high quality, low-cost Earth observation data for terrain mapping, disaster monitoring and climate change studies. ALOS has three remote sensing instruments, namely, the Panchromatic Remote-sensing Instrument for Stereo Mapping (PRISM) for digital elevation mapping, the Advanced Visible and Near Infrared Radiometer type2 (AVNIR-2) for precise land coverage observation, and the Phased Array type L-band Synthetic Aperture Radar (PALSAR) for day-and-night and all-weather land observation (Figure 1).

The ALOS was designed with two advanced technologies: the first is the high speed and large data capture capacity, and the second is the accurate spacecraft position and attitude determination capability - using an onboard GPS receiver and high precision star trackers to determine position and attitude with a high accuracy.

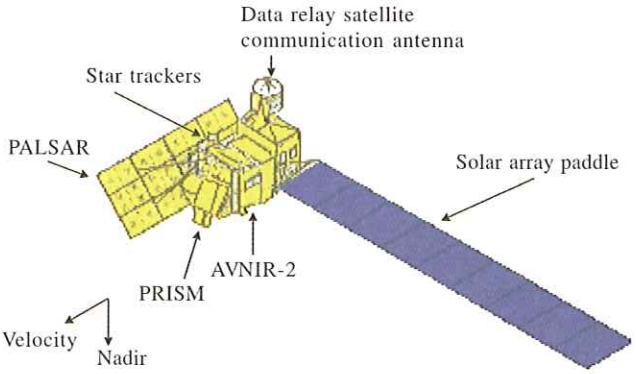

Figure 1. The ALOS satellite (*EORC JAXA*, 2006)

PALSAR provides better performance than the JERS-1's synthetic aperture radar (SAR). PALSAR operates in five observation modes: Fine Beam Single (FBS), Fine Beam Dual (FBD), Direct Transmission (DT), ScanSAR, and polarimetry (POL). It has finer spatial resolution (down to 10 metres in FBS mode) than JERS-1, with variable look angles.

In ScanSAR mode it is possible to acquire up to a 250 to 350 kilometres wide swath of SAR, but at the cost of spatial resolution. This swath is three to five times wider than conventional SAR images. PALSAR can provide global coverage three times per year in FBS/FBD mode and once a year in ScanSAR mode (EORC JAXA, 2006).

For InSAR applications, the coherence is an important

1082-4006/08/14(01)-12$5.00
©2008 The International Association of Chinese Professionals in Geographic Information Science (CPGIS)

parameter quantifying the accuracy of the interferometric measurements. The coherence can be affected by many factors, including geometric decorrelation, Doppler Centroid difference between the SAR images, impacts of volume scattering, temperature of sensors during data acquisition, temporal decorrelation, and so on (Zhang, Prinet, 2004). Unlike the C-band SAR sensor, the L-band PALSAR sensor is suitable for observations in vegetated areas. Temporal decorrelation can occur if there is a difference in the terrain (e.g. the trees lose their leaves, or snow covers the ground) between the two acquisitions, which can be caused by the change in weather or season. Low frequency radars with a longer wavelength (e.g. L-band SAR) are usually more sensitive to larger objects than high frequency radars (e.g. C-band SAR). Since it is easier for environmental effects to change/move smaller objects, the temporal decorrelation is expected to be a stronger affect for radars with shorter wavelength than radars with long wavelength (Ge, et al., 2007a; Ge, et al., 2004). Because of these factors, ALOS is expected to produce much more coherent SAR images than the JERS-1 and other previous C-band SAR satellites, which therefore makes it more suitable for DInSAR applications.

SAR has the remarkable ability of imaging the Earth's surface day or night, and even when the surface is cloud-covered. *This is particularly important for monitoring the Wenchuan quake because rains followed the main shock and most quake-stricken regions were covered by clouds.* The advantage of monitoring crustal deformation using a SAR-based remote sensing system is its large spatial coverage and cost effectiveness. In particular it is possible to investigate areas affected by large-scale seismic events.

Satellite differential SAR interferometry has been widely accepted as a powerful tool to map co-, post- and inter-seismic deformation since its successful applications to the 1992 Landers Earthquake (e.g. Massonnet, et al., 1993; Massonnet, et al., 1994; Massonnet, et al., 1996; Jonsson, et al., 2002; Jonsson, et al., 2003; Fialko, et al., 2005; Fialko, 2006; Wang, et al., 2007).

A few studies using PALSAR data for co-seismic deformation monitoring have been reported since the launch of ALOS. Matsuoka (2006) demonstrated ALOS's ability to monitor areas damaged by earthquake activity by comparing the correlation coefficient of a pre-event images pair and a pair of images spanning the seismic event (Matsuoka, 2006; Ge and Yonezawa, 2004). The results correlate well with the damage assessment reports from field survey and high-resolution optical satellite data. Results of co-seismic deformation from InSAR measurements using PALSAR data have also been reported. PALSAR data acquired before and after an earthquake can be used to detect the co-seismic deformation using the DInSAR technique. Ground surveys have been carried out to verify the results. The measured deformations are compared to those induced from a fault model and they are highly correlated (Miyagi, et al., 2007).

The aim of this study was to investigate the co-seismic deformation due to the most recent Wenchuan quake by satellite radar interferometry using ALOS/PALSAR data.

II. RESULTS FROM DIFFERENTIAL SAR INTERFEROMETRY

In order to map co-seismic deformation, PALSAR images for each path acquired before the quake must exist. As shown in Figure 2, the full Wenchuan fault is so long that it has to be covered with ALOS/PALSAR acquisitions from seven adjacent paths/tracks. In the figure the SRTM digital elevation model (Farr & Kobrick, 2000) was plotted as background. The location of the main quake is indicated by the star.

Fortunately, this indeed is the case so that as soon as a post-seismic PALSAR image was acquired, co-seismic deformation can be derived in near real-time (i.e. within 24 hours of image capture) from the pair formed with the pre- and post-seismic SAR images. The first post-seismic PALSAR acquisition occurred on 19 May 2008 from Path 473. At the time this paper was prepared, a second acquisition happened on 24 May 2008 from Path 476. Path 476 covers the epicentre, while Path 473 covers the worst-hit Beichuan City. This paper will focus on results generated from the co-seismic pairs from both paths.

Figure 3 shows the DInSAR results from ALOS/PALSAR co-seismic pairs from Paths 473 (17 February - 19 May) and 476 (8 April - 24 May). It can be seen clearly that the quake was so powerful, and hence the devastation was so widespread, that the SAR coverage appeared to be limited and several images from the same path are needed in order to include areas of least impact, which can be used as reference for phase unwrapping. For example, from the result it can be seen that the ground surface at the bottom right corner of Path 473 was displaced the least but a few more frames of images further down are needed in order to find a stable reference point.

Also obvious is the much better coherence n the Sichuan Basin at the bottom right half than in the mountainous region at the top left half. By zooming in on the top left portion of the interferograms, it is evident that topographic residuals exist in the DInSAR results because of the poor quality of the SRTM 3 arcsecond DEM in the rough terrain (Chang, et al., 2004). These results can be improved significantly by using a more accurate and higher resolution DEM equivalent to that of the PALSAR image, i.e. 10m.

Note also that the low spatial frequency fringes in the lower part of Path 473 interferogram. They are so similar to orbit fringes that only when DInSAR results from neighbouring paths, i.e. 472 and 474, become available can they be ascertained as true deformation.

On the other hand, the terrain was deformed so much along the fault, where the aftershocks are located, that fringes were

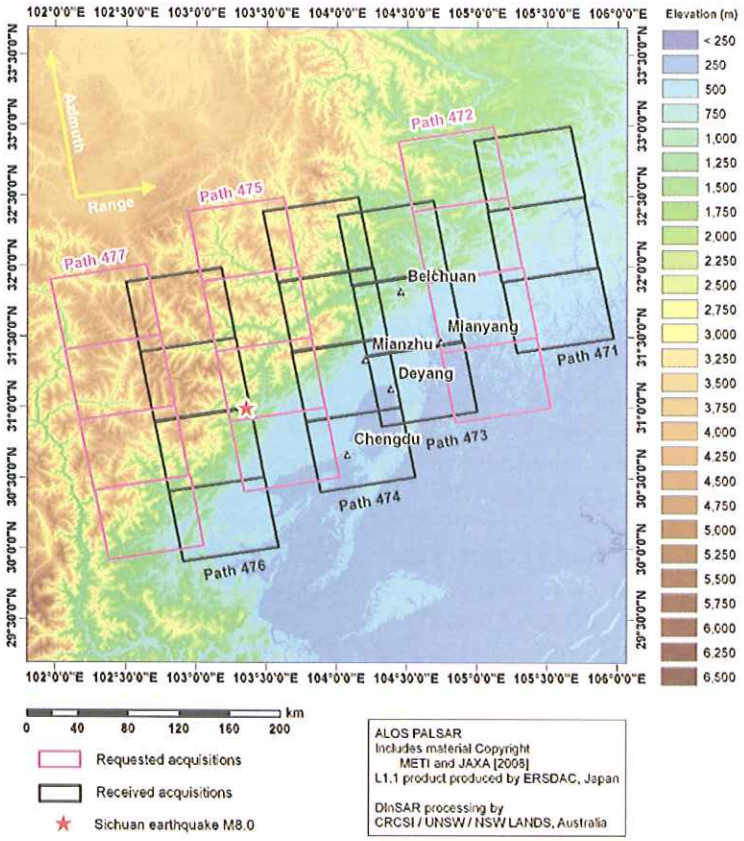

Figure 2. ALOS/PALSAR coverage of the Wenchuan seismic fault

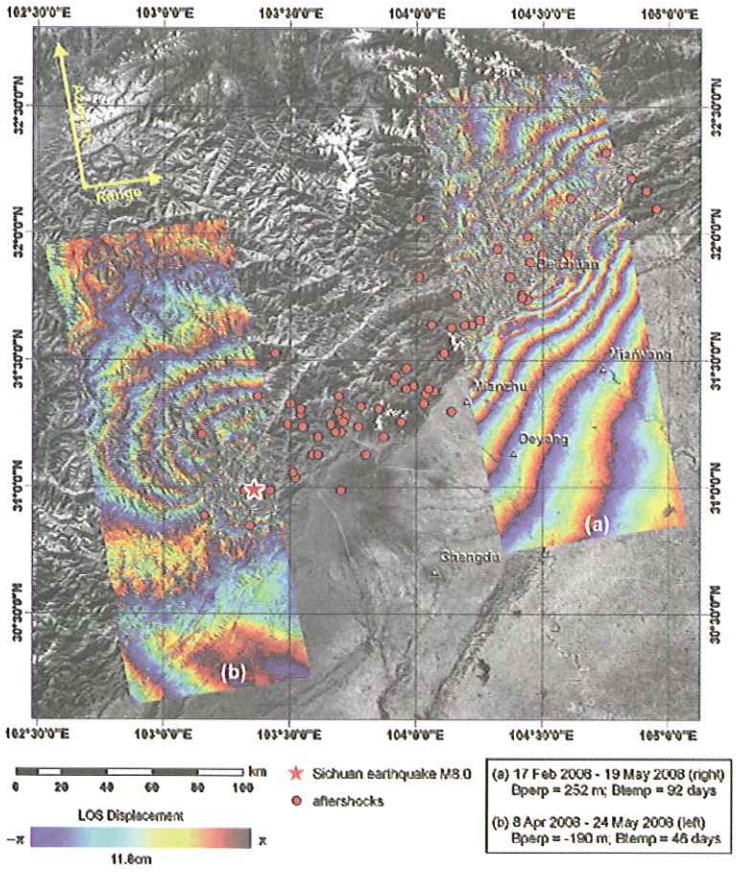

Figure 3. DInSAR results for Paths 473 and 476 overlaid on Landsat image

totally lost. This signal saturation (Ge, et al., 2007b) would lead to co-seismic deformation being underestimated, as shown in Figure 4.

Figure 4 shows RELATIVE ground movement in the radar-looking direction for each path from unwrapping interferograms of Paths 473 and 476. From this figure it is estimated that the ground surface displaced a maximum of 75cm and 130cm away from and towards the satellite respectively. But preliminary modelling results from seismic observations indicate around 5m displacement (Qiao, 2008). Therefore, other techniques such as pixel offset analysis have to be applied in order to resolve large displacement of the order of a few metres along the fault, while DInSAR is used as a highly accurate technique (~cm level) with limited dynamic range (~1-2m) (Ge et al., 2007a).

III. RESULTS FROM PIXEL OFFSET ANALYSIS

In order to measure large ground displacement along the fault, pixel offset analysis (Wang, et al., 2007; Tobita, et al., 2001) was carried out in order to calculate ground surface movement in both the azimuth and range directions. Satellite radar scans an area of interest in both the satellite flight direction (i.e. azimuth direction) and the radar looking direction (i.e. slant range direction). The range and azimuth offsets are first estimated using the intensity cross-correlation method for each grid of approximately 16 and 32 pixels respectively. Over-sampling of the correlation function between the images is done in order achieve sub-pixel level accuracy (better than 0.2 pixels). A quadratic polynomial is then used to remove trends in the estimated offsets in order to obtain the range/azimuth residuals. These residuals are then converted to ground surface displacement in both azimuth and range directions.

Figure 5 shows the results of pixel offset analysis for azimuth (left) and range (right). Comparing Figure 5(b) with Figure 4(b) it can be seen that the two agree well with each other in general, but pixel offset analysis reveals much larger ground displacement around the epicentre of the Ms 8.0 main shock, where the DInSAR signal is saturated. Hence pixel offset analysis can be used as a technique in cases of large dynamic range to complement DInSAR results.

On the other hand, there are difficulties to fully explain the azimuth result. One possible explanation is that differential atmospheric delay has caused the pattern (Janssen, et al., 2004; Xu, et al., 2006). Therefore, in Figure 6 only range offset results for both paths were collocated.

IV. RESULTS FROM COHERENCE DIFFERENCE

Coherence map is a by-product of the radar interferometry and measures the similarity between two radar images. In general, the coherence between the two images taken before

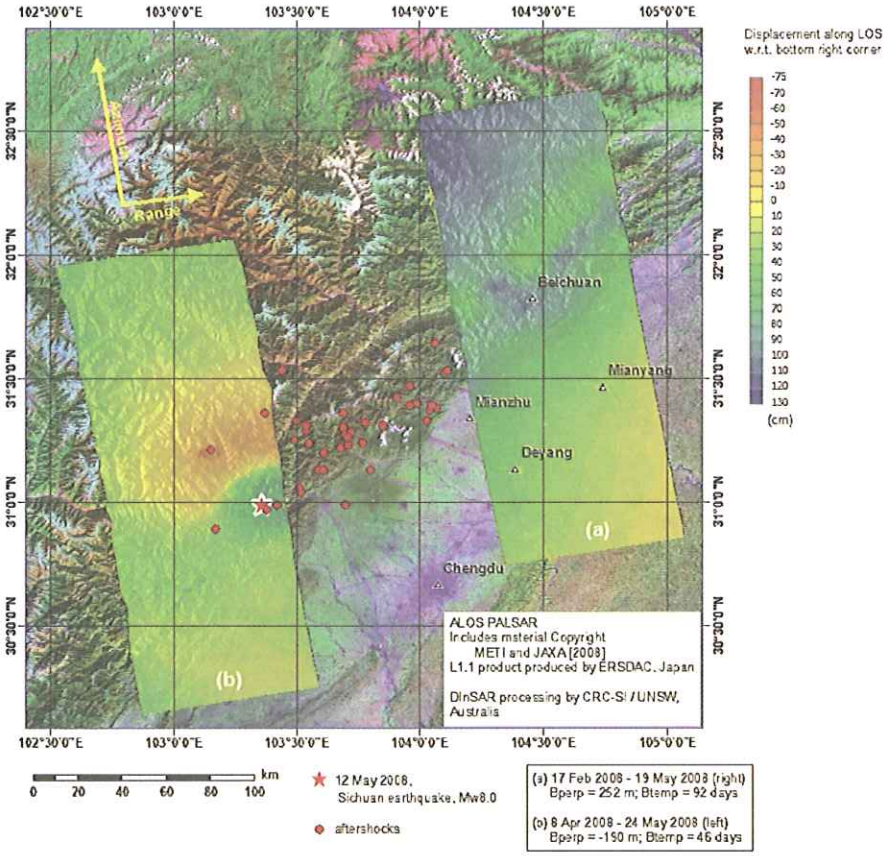

Figure 4. Line-of-sight displacement from unwrapping interferograms in Figure 3

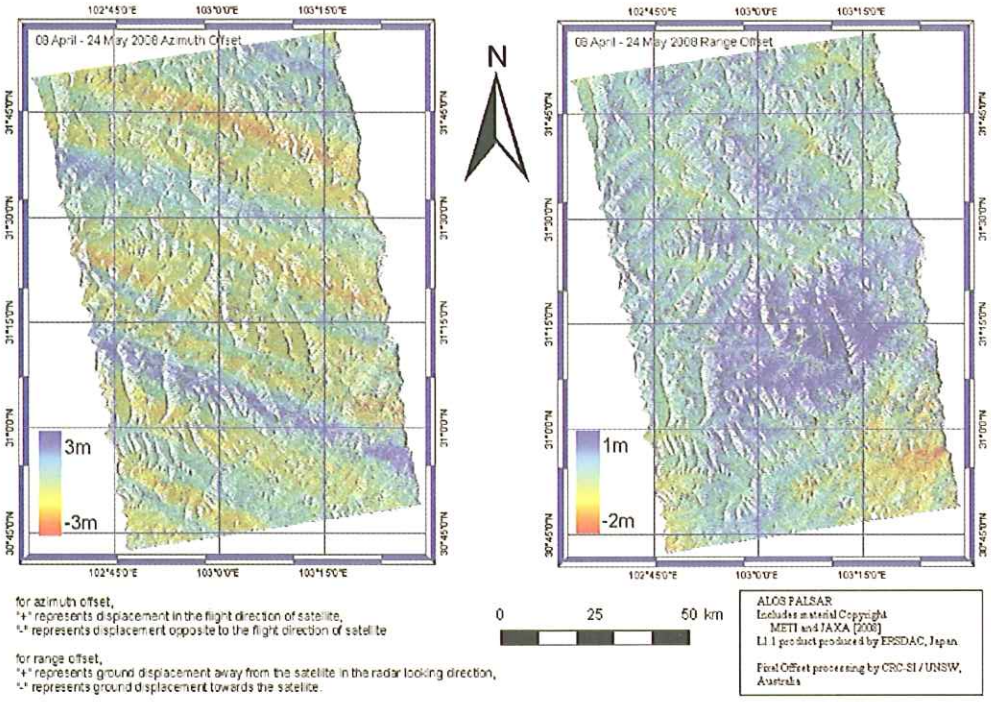

Figure 5. Ground displacement map from pixel offset analysis for Path 476: a) in azimuth direction and b) in range direction

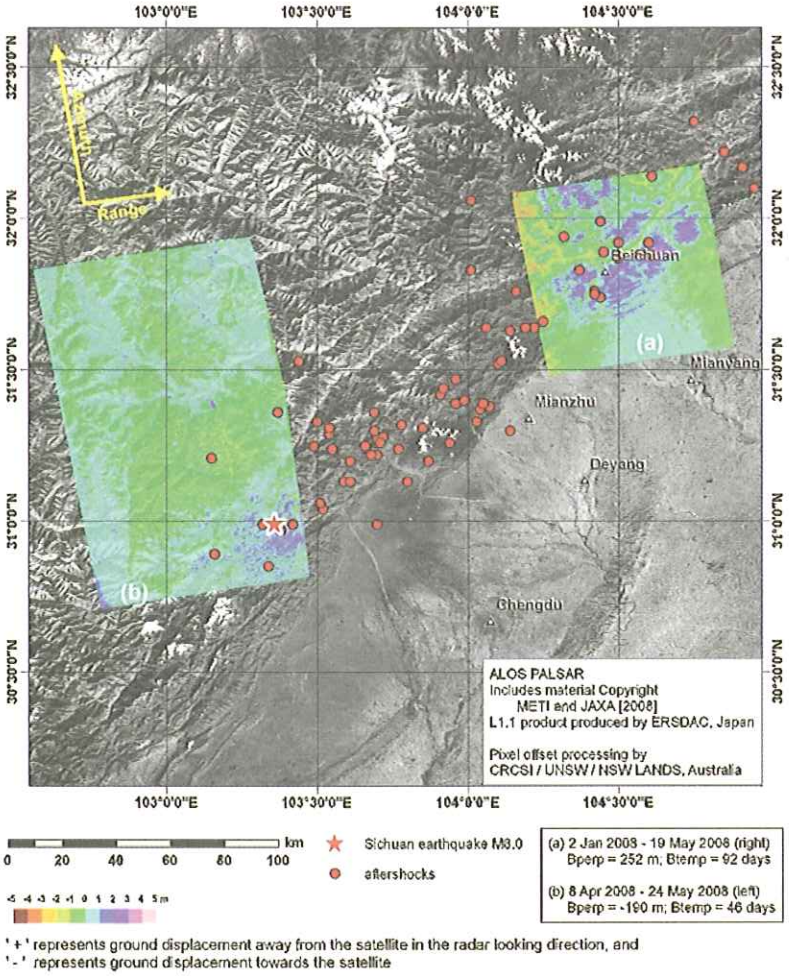

Figure 6. Ground displacement map from pixel offset analysis from Paths 476 and 473 (range only)

the quake, namely 2 January and 17 February acquisitions for Path 473, is high. On the other hand, the coherence between one image taken before the quake, 17 February acquisition, and one taken after the quake, i.e. 19 May acquisition, is reduced in damaged areas and remains high in undamaged regions. Therefore, the difference between the two coherence maps, namely (2 January and 17 February)—(17 February and 19 May), represents the level of quake-induced damage (Matsuoka, 2006; Ge, Yonezawa, 2004).

Figure 7 shows the quake damage assessment based on the difference of DInSAR coherence for Path 473. In the figure, 0.7 represents severe damage (hence rescue is most needed); 0.0 means no damage (location can be used as safe island); and –0.4 means rubble accumulated in the location (indicating possible blockage of roads and river channels). Figure 8 presents a similar result for Path 476.

V. CONCLUDING REMAKES AND FUTURE WORK

Preliminary results of satellite radar differential interferometry for the co-seismic deformation of the 12 May 2008 Ms8.0 Wenchuan Earthquake were derived from ALOS/PALSAR data for Paths 473 and 476, with two images acquired before the quake and one after the event for each path. Three products were described in this paper. Among them, the DInSAR result is highly accurate but with limited dynamic range. Pixel offset analysis can be used as a technique in cases such as this where there is large dynamic range, to complement DInSAR. The difference of coherence between pre- and co-seismic pairs, a by-product of DInSAR, can be used for quantitative quake damage assessment.

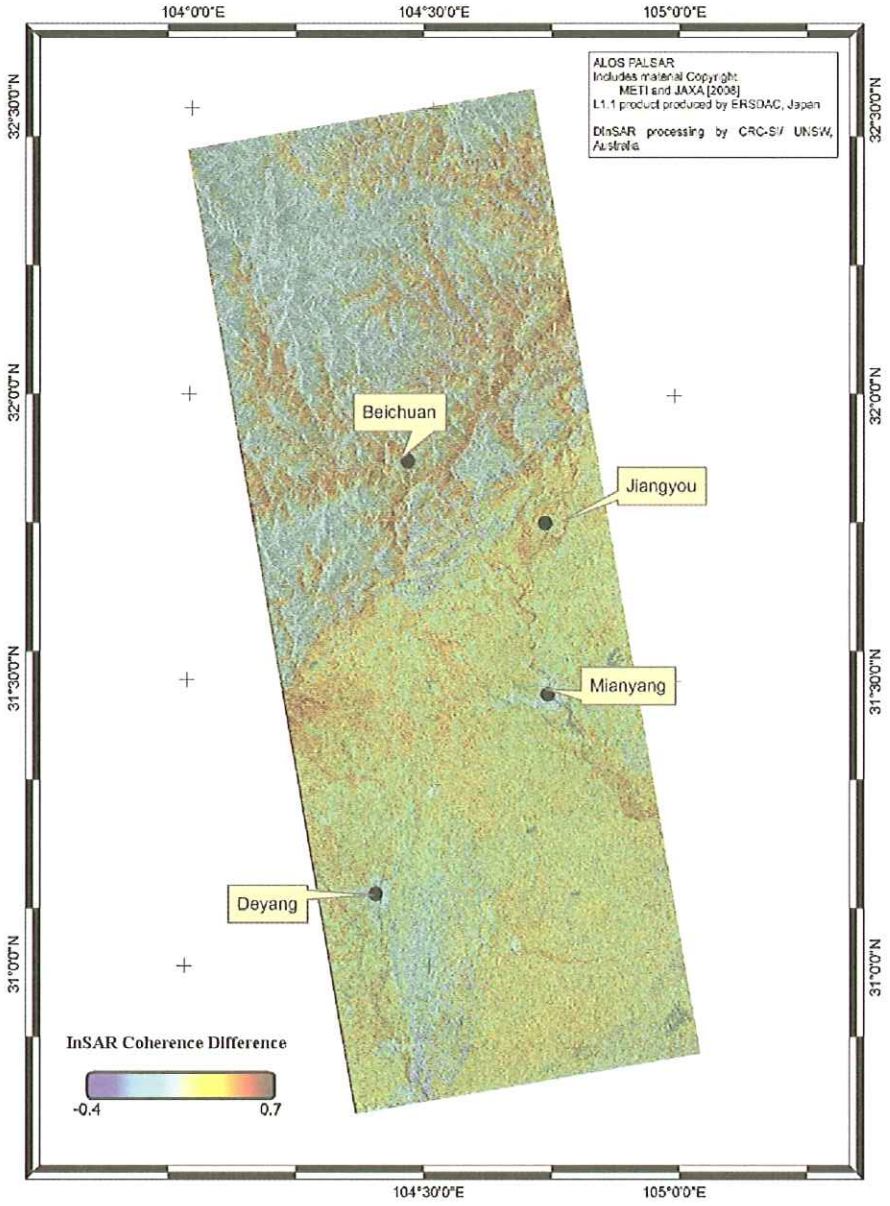

Figure 7. Coherence difference between pre- and co-seismic pairs for Path 473

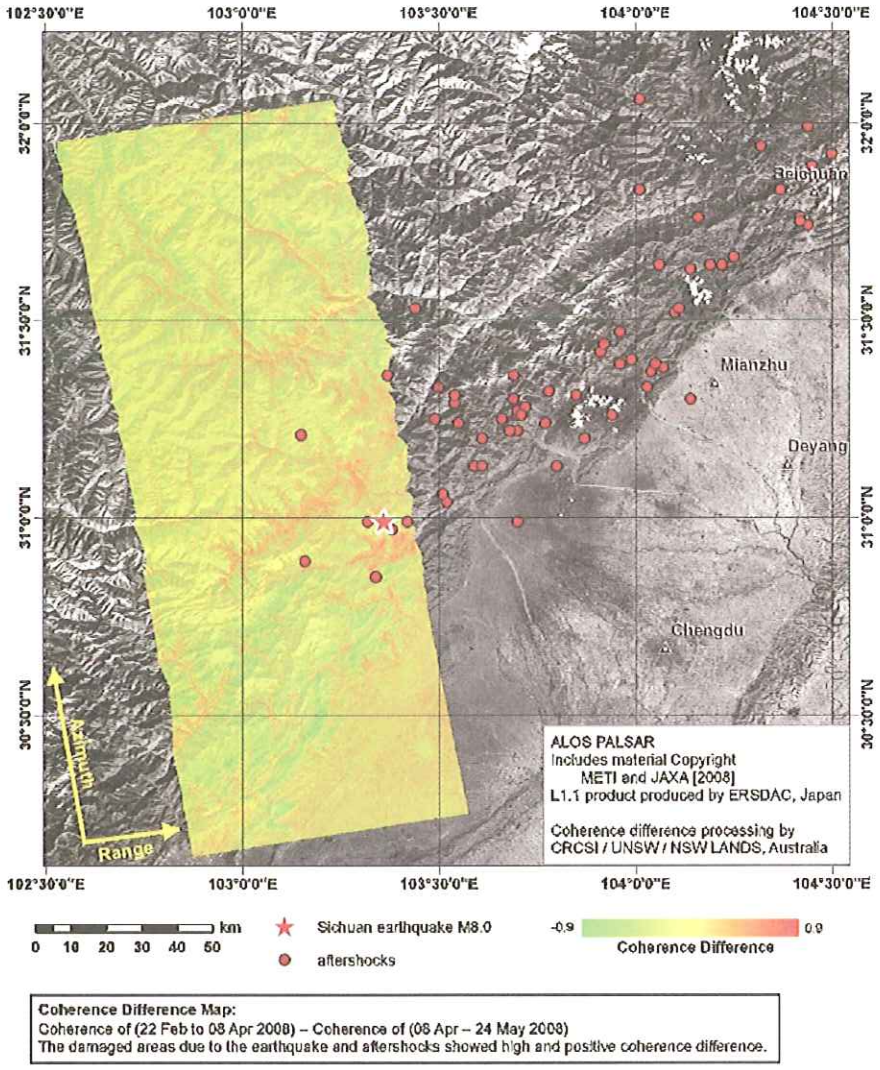

Figure 8. Coherence difference between pre- and co-seismic pairs for Path 476

In addition to refining the preliminary results reported here, future work will include:

- Mapping the whole seismic fault;
- Inverse modelling of the co-seismic deformation from both DInSAR and pixel offset analysis, and comparing these with results from seismic observation;
- Comparing SAR observed co-seismic deformation with ground survey results; and
- Correlating coherence difference with damage assessment from survey on the ground.

ACKNOWLEDGEMENT

This research work has been supported by the Cooperative Research Centre for Spatial Information through Project 4.09, whose activities are funded by the Australian Commonwealth's Cooperative Research Centres Programme. The Australian Research Council and the Australian Coal Association Research Program have been funding radar related studies of the team in the last few years.

We wish to thank the Earth Remote Sensing Data Analysis Center (ERSDAC) for providing ALOS PALSAR data. We also acknowledge the strong support from the International Association of Geodesy Sub-Commission 4.4 "Applications of Satellite & Airborne Imaging Systems" and the IAG Consortium for Mine Subsidence Monitoring.

METI and JAXA have the ownership of the ALOS PALSAR original data. The PALSAR Level-1.1 products were produced and provided to the CRC-SI/UNSW by ERSDAC, Japan.

The authors wish to thank Prof Hui Lin of the Chinese University of Hong Kong for providing the opportunity to publish the preliminary results in such a timely manner.

REFERENCES

[1] Chang H C., L. Ge, C. Rizos, 2004. Assessment of digital elevation models using RTK GPS. *Journal of Geospatial Eng*, 6

(1): 13—20.

[2] China Earthquake Administration (CEA), 2008. http://ww.cea.gov.cn:99/manage/html/8a8520ba1a04b8f0011a04cdf6970004/index.html, last accessed on 10/06/2008.

[3] China Seismic Information Network (CSIN), 2008. http://www.csi.ac.cn/sichuan/sichuan080512_his.htm, last accessed on 10/06/2008.

[4] EORC JAXA, 2006, About ALOS, EORC JAXA, http://www.eorc.jaxa.jp/ALOS/about/about_index.htm, last accessed on 10/12/2007.

[5] Farr, T., M. Kobrick, 2000. Shuttle Radar Topography Mission produces a wealth of data. *AGU Eos* 81: 583—585.

[6] Fialko Y., 2006, Interseismic strain accumulation and the earthquake potential on the southern San Andreas fault system. *Nature*, 441(7096): 968—971.

[7] Fialko Y., D. Sandwell, M. Simons, P. Rosen, 2005, Three-dimensional deformation caused by the Bam, Iran, earthquake and the origin of shallow slip deficit. *Nature*, 435(7040): 295—299.

[8] Ge L., C. Yonezawa, 2004, Radar interferometry for disaster prevention and mapping, pres. *International Workshop on Earth Observation Technology and Application* (CEOS 2004), November 16—17, Beijing, China (invited presentation).

[9] Ge L., H C. Chang, C. Rizos, 2007a, Mine subsidence monitoring using multi-source satellite SAR images. *Photogrammetric Engineering and Remote Sensing*, 73(3): 259—266.

[10] Ge L., H. Wang, H C. Chang, 2007b, Linear combination for differential radar interferometry. *The XXIV General Assembly of the International Union of Geodesy and Geophysics* (IUGG 2007), Perugia, Italy, 2—13 July.

[11] Ge L., X. Li, C. Rizos, M. Omura, 2004, GPS and GIS assisted radar interferometry. *Photogrammetric Engineering and Remote Sensing*, 70(10): 1173—1178.

[12] Janssen V., L. Ge, C. Rizos, 2004, Tropospheric corrections to SAR interferometry from GPS observations. *GPS Solutions*, 8 (3): 140—151.

[13] Jónsson S., H. Zebker, P. Segall, 2002, Fault slip distribution of the 1999 Mw7.1 Hector Mine, California, earthquake, estimated from satellite radar and GPS measurements. *Bulletin of the Seismological Society of America*, 92(4): 1377—1389.

[14] Jonsson S., P. Segall, R. Pedersen, G. Bjornsson, 2003, Post-earthquake ground movements correlated to pore-pressure transients. *Nature*, 424(6945): 179—183.

[15] Massonnet D., et al., 1993, The displacement field of the Landers earthquake mapped by radar interferometry. *Nature*, 364(6433): 138—142.

[16] Massonnet D., K. Feigl, M. Rossi, F. Adragna, 1994, Radar interferometric mapping of deformation in the year after the Landers earthquake. *Nature*, 369(6477): 227—230.

[17] Massonnet D., Thatcher W., Vadon, H., 1996, Detection of postseismic fault-zone collapse following the Landers earthquake. Nature, 382(6592): 612—616.

[18] Matsuoka, M., 2006, Use of ALOS/PALSAR imagery for monitoring areas damaged due to recent natural disasters, disaster forewarning diagnostic methods and management. *Proc. of SPIE*, Vol.6412, ID641204, 2006.11.

[19] Miyagi Y., Y. Nishimura, H. Takahashi, M. Shimada, 2007, Crustal deformation caused by earthquake detected by InSAR technique using ALOS/PALSAR data. *Eos Trans. AGU*, 88(52): Fall Meet. Suppl.

[20] Qiao X., 2008, Personal communications.

[21] Tobita M., M. Murakami H. Nakagawa H., et al., 2001, 3-D surface deformation of the 2000 Usu eruption measured by matching of SAR images. *Geophysical Research Letter*, 28(22): 4291—4294.

[22] Wang H., L. Ge, C. Xu, 2007, 3-D coseismic displacement field of the 2005 Kashmir earthquake inferred from satellite radar imagery. *Earth Planets & Space*, 59(5): 343—349.

[23] Wang H., C. Xu, L. Ge, 2007, Coseismic deformation and slip distribution of the 1997 mw7.5 Manyi, Tibet, earthquake from InSAR measurements. *Journal of Geodynamics*, 44(3—5): 200—212.

[24] Xu C., H. Wang, L. Ge, C. Yonezawa, P. Cheng, 2006, InSAR tropospheric delay mitigation by GPS observations: A case study in Tokyo area. *Journal of Atmospheric and Solar-Terrestrial Physics*, 68(6): 629—638.

[25] Zhang Y., V. Prinet, 2004, InSAR coherence estimation. *Geoscience and Remote Sensing Symposium (IGARSS 2004 Proceedings)*, September 20—24, 5: 3353—3355.